

Developmental IL-6 Exposure Favors Production of PDGF-Responsive Multipotential Progenitors at the Expense of Neural Stem Cells and Other Progenitors

Ekta Kumari,^{1,3} Fernando J. Velloso,^{1,3} Azadeh Nasuhidehnavi,¹ Aditya Somasundaram,¹ Vibha H. Savanur,¹ Krista D. Buono,² and Steven W. Levison^{1,*}

¹Department of Pharmacology, Physiology and Neuroscience, Rutgers Biomedical Health Sciences of Rutgers University, 205 South Orange Ave. Newark, NJ 07103, USA

²ICON Laboratory Services, Farmingdale, NY 11735, USA

³Co-first author

*Correspondence: levisosw@rutgers.edu

<https://doi.org/10.1016/j.stemcr.2020.03.019>

SUMMARY

Interleukin-6 (IL-6) is increased in maternal serum and amniotic fluid of children subsequently diagnosed with autism spectrum disorders. However, it is not clear how increased IL-6 alters brain development. Here, we show that IL-6 increases the prevalence of a specific platelet-derived growth factor (PDGF)-responsive multipotent progenitor, with opposite effects on neural stem cells and on subsets of bipotential glial progenitors. Acutely, increasing circulating IL-6 levels 2-fold above baseline in neonatal mice specifically stimulated the proliferation of a PDGF-responsive multipotential progenitor accompanied by increased phosphorylated STAT3, increased *Fbxo15* expression, and decreased *Dnmt1* and *Tlx* expression. Fate mapping studies using a Nestin-CreERT2 driver revealed decreased astrogliogenesis in the frontal cortex. IL-6-treated mice were hyposmic; however, olfactory bulb neuronogenesis was unaffected. Altogether, these studies provide important insights into how inflammation alters neural stem cells and progenitors and provide new insights into the molecular and cellular underpinnings of neurodevelopmental disorders associated with maternal infections.

INTRODUCTION

A large number of studies support the view that maternal infection, or maternal immune activation (MIA), is a significant contributor to the pathology of autism spectrum disorders (ASD) (Atladottir et al., 2010; Zerbo et al., 2015). Indeed, a recent study of more than 2 million Swedish women found that having an infection during pregnancy increased the risk of having a child with autism by 37% (Lee et al., 2015). Observations in ASD and models of MIA (Smith et al., 2007) are analogous to those seen in fetal inflammatory response syndrome, where one of the diagnostic markers is an increase in interleukin-6 (IL-6) concentration (Gomez et al., 1998). In particular, studies have established that the levels of IL-6 are increased in maternal serum, amniotic fluid, and serum of children subsequently diagnosed with ASD (Ashwood et al., 2011; Croonenberghs et al., 2002). Moreover, independent studies have established that children and adults with ASD have higher circulating IL-6 levels compared with controls (Ashwood et al., 2011). These increases are associated with irritability, impaired communication and sociabilization skills and intelligence. Accordingly, IL-6 is increasingly being used as a biomarker for ASD (Yang et al., 2015).

Infections in pregnant mice and rats, can be mimicked by administering agents that activate the maternal immune system, such as maternal injections of the synthetic double-stranded RNA poly(I:C) (to evoke an anti-viral inflam-

matory response) or by administering lipopolysaccharide (LPS) (to evoke an anti-bacterial inflammatory response). These immune activators increase circulating levels of cytokines, including IL-6 (Kirsten et al., 2018) that can cross the placenta and the fetal blood-brain barrier (Aaltonen et al., 2005; Zaretsky et al., 2004) to affect the developing brain (Wu et al., 2017). Studies in mice have shown that these immune activators elicit many of the cardinal behavioral features of autism, as well as neuropathological aberrations (Malkova et al., 2012; Smith et al., 2007). However, it is not clear how these cytokines alter the trajectory of neural development.

At present, the majority of animal models of MIA used to study autism have manipulated the maternal immune system at time points that correspond to the first trimester of human development (Malkova et al., 2012; Meyer et al., 2006; Smith et al., 2007). Such studies will affect the primitive neural stem cells (NSCs) and neural stem and progenitors (NSPs) that reside in the neuroepithelium known as the ventricular zone (VZ). However, epidemiological studies on ASD have shown associations between maternal infections in the late second trimester and early third trimester and incidence of ASD (Zerbo et al., 2015), when proliferative cells in the VZ are declining in number, and the subventricular zone (SVZ) is expanding rapidly to peak in size during early postnatal development. Mice are born precociously, thus the brain of a newborn mouse is equivalent to that of an early third-trimester human infant



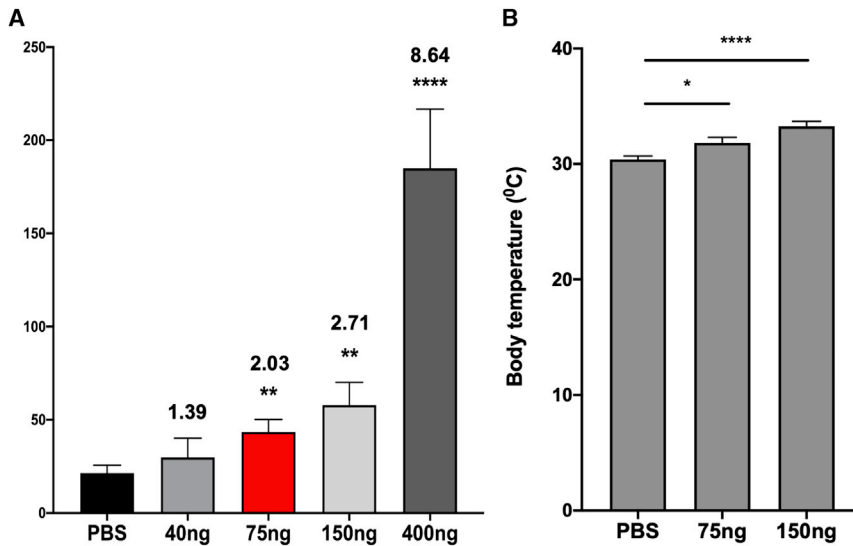


Figure 1. Systemic rmIL-6 Administration Increases Blood Plasma Concentration of IL-6 and Body Temperature

(A) Blood plasma levels of IL-6 in pg/mL measured by ELISA in groups of at least six mice that received different doses of rmIL-6 or PBS. Error bar indicates SEM from three independent experiments. ** $p < 0.01$, **** $p < 0.0001$ using Student's *t* test. $n = 6$. (B) Mice body temperature measured 1 h after the last rmIL-6 injection. Numbers over bars represent fold change over PBS group. Error bar indicates SEM from three independent experiments. * $p < 0.05$, **** $p < 0.0001$ using Student's *t* test. $n = 12$ mice.

(Salmaso et al., 2014). Therefore, to model the effects of maternal inflammation in mice using a more appropriate animal model, we manipulated the levels of IL-6 in the neonatal mouse and asked how this affected the pool of NSCs and progenitors in the SVZ of the forebrain.

RESULTS

Modeling Maternal Infections by Systemically Injecting IL-6

Previous studies have measured 2- to 3-fold increases in the blood plasma IL-6 levels in children with ASD (Ashwood et al., 2011). Therefore, to determine the dose of IL-6 needed to mimic the increased levels of IL-6 seen in children who will develop ASD, we injected neonatal mice with four doses of IL-6 (40, 75, 150, and 400 ng) versus PBS twice on postnatal day 4 (P4) and once on P5 and then measured plasma levels of IL-6 2 h after the third injection. We used this paradigm to produce sustained increased levels of IL-6 for at least 36 h. Mice that received 40 ng of recombinant mouse IL-6 (rmIL-6) had blood plasma levels of 31 ± 10 pg/mL versus 21 ± 4.3 pg/mL in PBS-injected littermates (1.4-fold increase). Mice that received 75 and 150 ng had blood plasma levels of 43 ± 6.7 pg/mL (2-fold increase) and 58 ± 12 pg/mL (2.7-fold increase) of IL-6, respectively. Finally, mice that received 400 ng IL-6 had 185 ± 32 pg/mL in blood plasma (8.6-fold increase) (Figure 1A; Table S1). The doses of 75 and 150 ng of IL-6 resulted in blood plasma levels similar to those observed in ASD children. To determine whether these doses were eliciting a systemic response, we measured the body temperature of mice that received 75 and 150 ng of IL-6 1 h after the last injection. The 2- to 3-fold increase

in circulating IL-6 caused a small but significant increase in body temperature (Figure 1B). We decided to use 75 ng of IL-6 for subsequent *in vivo* studies, as it elicited a systemic response inside the range of the blood plasma levels observed in ASD children (Ashwood et al., 2011).

Elevated Level of IL-6 Increases the Proliferation of PDGF-Responsive Multipotential Progenitors *In Vivo*

We hypothesized that systemically elevating IL-6 would directly affect the NSPs in the developing mouse brain. Using a multi-marker flow panel comprised of CD133/CD140a/NG2/LeX, we have previously established that there are seven subsets of neural progenitors as well as NSCs in the neonatal mouse SVZ (Buono et al., 2012). When isolated by fluorescence-activated cell sorting (FACS) these NSCs and progenitors have different potentialities and growth factor responsiveness *in vitro* (Table S2). To establish how increased levels of IL-6 would affect these NSPs individually *in vivo*, we injected 75 ng of IL-6 twice on P4 mice and once on P5 mice (Figure 2A) and analyzed changes in NSP proliferation using ethynyl deoxyuridine (EdU) incorporation. EdU (50 mg/kg) was injected twice at intervals of 2 and 4 h before euthanizing the mice for flow cytometry. The gating scheme for the flow cytometry is shown in Figures 2B and 2C. A significant increase was detected in the proliferation of the platelet-derived growth factor (PDGF) and fibroblast growth factor 2 (FGF-2)-responsive multipotential progenitors (PFMPs) (Figure 2D; PBS: $8.6\% \pm 3.45\%$, IL-6: $22.2\% \pm 5.32\%$; $p < 0.05$) compared to controls. However, there was no significant change in EdU incorporation into other SVZ cells (NSC, PBS: $14.6\% \pm 9.09\%$, IL-6: $15.45\% \pm 8.94\%$; multipotential progenitor-1 [MP1], PBS: $6.96\% \pm 3.37\%$, IL-6: $7.76\% \pm$

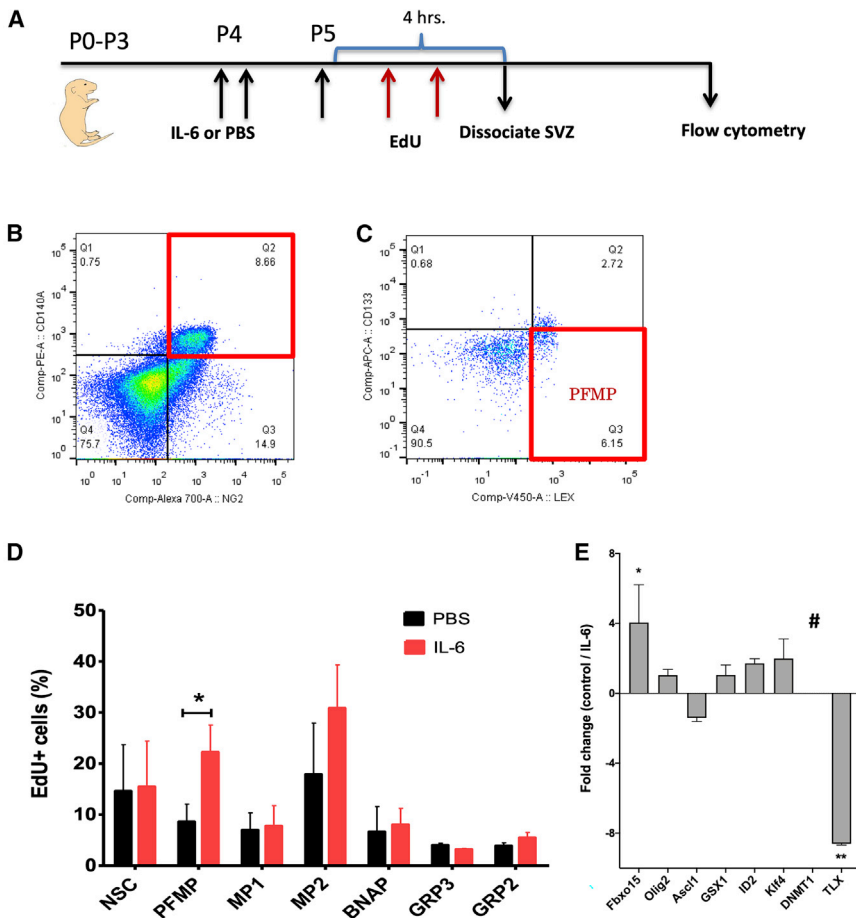


Figure 2. IL-6 Signals to SVZ Cells and Alters the Proliferation of PDGF-Responsive Multipotential Progenitors of SVZ *In Vivo* (A) Schematic of *in vivo* analysis of effects of IL-6 on EdU incorporation into stem cells and progenitors.

(B) Gating strategy for flow cytometry.

(C) Boxplots of flow cytometry data for PFMPs.

(D) Multicolor flow cytometric analysis of pups injected with 75 ng of rmIL-6 on P4 and P5 followed by 50 mg/kg EdU on P5. IL-6 increased EdU incorporation into PFMPs significantly, but not into other SVZ cell types. Data are averaged from three independent experiments. Error bar indicates SEM. * $p < 0.05$ using Student's t test. $n = 12$ male mice. NSC, neural stem cell; PFMP, PDGF/FGF-2-responsive multipotential progenitors; MP, multipotential progenitor; BNAP, bipotential neuronal and astrocytic-associated progenitor; GRP, glial-restricted progenitor.

(E) PFMPs were sorted from neurospheres that been treated with 5 ng/mL IL-6 or PBS. Data are presented as fold change from the control group. Error bars represent SEMs from three independent experiments. * $p < 0.05$, ** $p < 0.01$ using Student's t test comparing IL-6-treated samples with untreated controls.

3.98%; MP2, PBS: 17.88% \pm 10.03%, IL-6: 30.83% \pm 8.47%; bipotential neuron astrocyte progenitor [BNAP], PBS: 6.64% \pm 4.94%, IL-6: 7.99% \pm 3.23%; glial-restricted progenitor 3 [GRP3], PBS: 4% \pm 0.40%, IL-6: 3.19% \pm 0.22%; GRP2, PBS: 3.88% \pm 0.61%, IL-6: 5.48% \pm 0.99%.

IL-6 Alters Gene Expression of PFMPs *In Vitro*

Whereas others have described PDGF-responsive multipotential progenitors, to date there is very little known about their transcriptome. Therefore, to begin to understand which transcription factors might be involved in the increase in PFMPs, neurospheres were established *in vitro* and PFMPs were sorted as described above. Sorted PFMPs were cultured for 24 h, and then treated with IL-6 (5 ng/mL) and soluble IL-6 receptor (sIL-6R) (5 ng/mL) for 2 h before RNA extraction and qPCR. IL-6 significantly increased the expression of the transcription factor *Fbxo15* (Fc 4.1 \pm 2.1, $p < 0.05$), while conversely decreasing the expression of *Tlx* (Fc -8.6 \pm 0.1, $p < 0.01$) and lowered the expression levels of *Dnmt1* below detection levels (Figure 2E).

SVZ NSPs Express Both GP130 and IL-6R

As we saw changes in the proliferation of specific NSP subsets in response to IL-6, we asked whether the NSPs express GP130 and IL-6 alpha receptor (IL-6R α), which comprise the IL-6R complex. Neurospheres were established from P5 mice, propagated for 7 days and then analyzed by western blot. As predicted, these NSPs expressed the IL-6R (68 kDa) and GP130 (130 kDa) receptor, as validated by comparing the NSPs with a macrophage cell line (Figure 3A). However, neurospheres are a complex mixture of progenitors and stem cells. Therefore, to establish more precisely which cells within the neurospheres express the IL-6R, we performed flow cytometry, combining antibodies to the IL-6R with the four other antibodies used to characterize the NSPs (Figure 3B). Spleen cells were used as a positive control for the expression of IL-6R. This analysis revealed that BNAP/GRP1, GRP2, MP4, PFMP, and MP2 express IL-6R, whereas receptor expression was below the level of detection for the NSCs, GRP3, and MP1 (Figure 3C). Altogether, these data demonstrate that most SVZ progenitors can be directly stimulated by the cytokine IL-6.

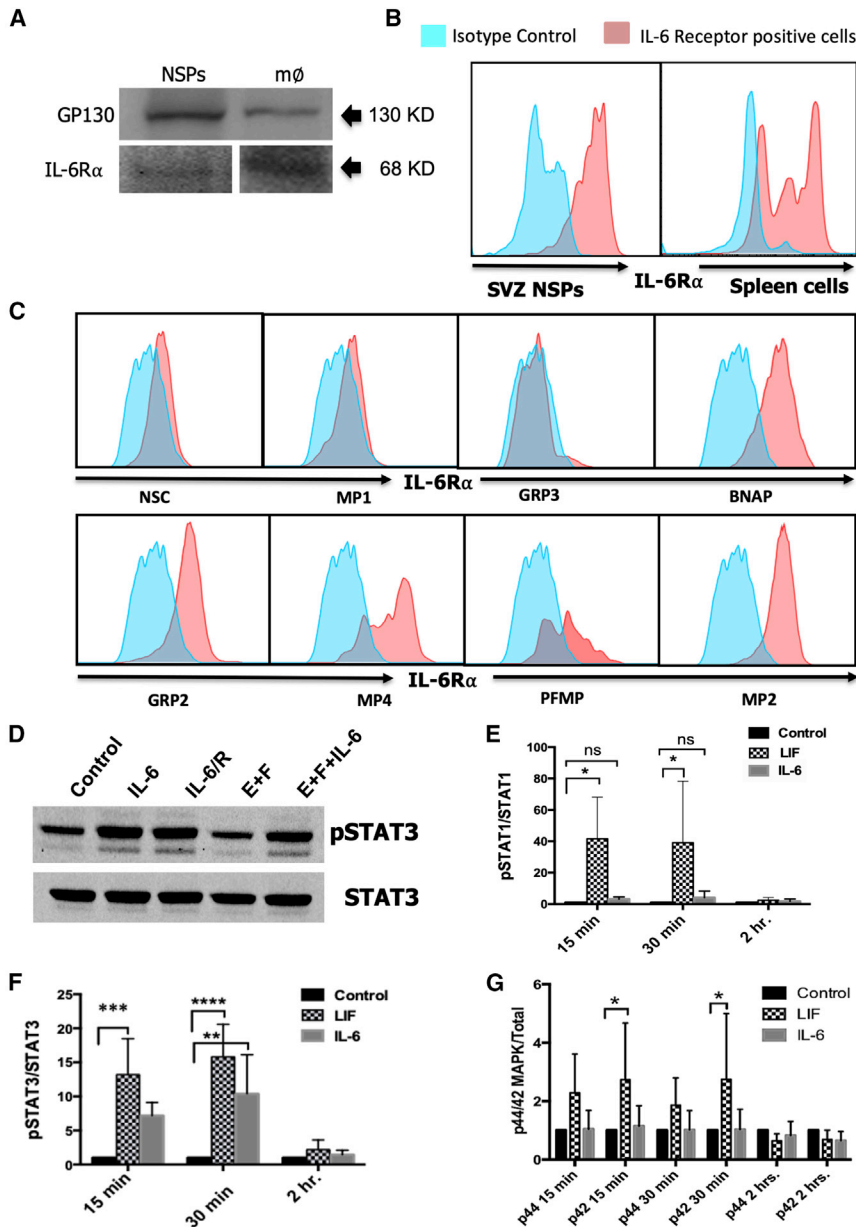


Figure 3. SVZ NSPs Express GP130 Receptor and the IL-6R α and IL-6 Activates pSTAT3 Signaling

SVZ NSPs from P5 mice were propagated as neurospheres for 7 days. The macrophage RAW 264.7 cell line (m ϕ) was used as a positive control.

(A) Representative blots for GP130 receptor (130 kDa) and IL-6R α (68 kDa) (see also Figure S1).

(B) SVZ NSP IL-6R α expression was evaluated by flow cytometry. Spleen cells were used as a positive control.

(C) Secondary neurospheres were dissociated and analyzed by multi-marker flow cytometry using a panel of antibodies comprised of anti-CD133/LeX/NG2/CD140a/IL-6R. A total of 50,000–100,000 live cells events were analyzed after excluding debris and dead cells using DAPI and gating on positively stained cells based on isotype controls. Data are representative of two independent experiments.

(D) Neurospheres from P4 mice propagated for 6 days were treated with 5 ng/mL of rmIL-6, rmIL-6 + 50 ng/mL of sIL-6R, 20 ng/mL of EGF + 10 ng/mL of FGF2, EGF + FGF2 + rmIL-6 + rmIL-6R for 30 min, then samples were analyzed for pSTAT3 and total STAT3. Time course study where samples were analyzed for the phosphorylation of STAT1 (E), STAT3 (F) and MAPK (G) at 15, 30, and 120 min after IL-6 addition. Data representative of three independent experiments. Values represent fold change \pm SEM. * p < 0.05, ** p < 0.01, as analyzed using ANOVA and Tukey's *post-hoc* test, n = 6.

IL-6 Activates pSTAT-3 in SVZ Neural Precursors in the Absence of sIL-6R Trans-signaling

IL-6 can activate downstream signaling in cells in absence of mIL-6R, via a phenomenon known as trans-signaling where sIL-6R associates with gp130; therefore, cells that do not express the IL-6R may still be affected by IL-6. Once the IL-6 binds to gp130 and to the IL-6R, it activates intracellular tyrosine kinases, such as the Janus kinases (JAKs), which then phosphorylate downstream signaling proteins that include Stat1 and Stat3, the RAS-RAF-MAPK pathway, and the phosphatidylinositol 3-kinase pathway. We investigated these downstream signal pathways upon stimulating SVZ

NSPs with IL-6 in the presence or absence of sIL-6R. As shown in Figure 3D, IL-6 strongly increased levels of pSTAT3 in the NSPs in the absence of trans-signaling. Interestingly, the related cytokine leukemia inhibitory factor (LIF) increased phosphorylation of both STAT3 and STAT1 (Figures 3E and 3F). A time course analysis revealed that IL-6 activated pSTAT3 significantly within 15 min of addition (p < 0.05), with further activation up to 30 min, achieving a \sim 7-fold increase (Figure 3F; p < 0.01) that returned to baseline within 2 h. The phosphorylation of other signaling proteins, such as pSTAT1, pMAPK, pAKT were not significantly affected by IL-6 addition (Figures 3E and 3G).



IL-6 Increases Tripotentiality in Neurospheres Containing PDGF-Responsive Progenitors, but Not in Neurospheres Enriched for NSCs

In previous studies, we reported that IL-6 increased the size, number, and self-renewal (beyond four passages) of rat SVZ NSPs compared with controls, which we interpreted as evidence that IL-6 increased the self-renewal of the NSCs (Covey et al., 2011). By contrast, propagating mouse SVZ NSPs at the same cell density and in a medium containing 20 ng/mL epidermal growth factor (EGF), 10 ng/mL FGF-2, and 5 ng/mL IL-6 for 7 days significantly decreased both the number and size of neurospheres formed (Figures 4A1–A3). This reduction was confirmed by dissociating the secondary neurospheres and analyzing the total number of live cells, which revealed a decrease in the total cell yield from neurospheres treated with IL-6 compared with control (IL-6: 1.4×10^6 versus control: 1.9×10^6). Staining these neurospheres for astrocyte (glial fibrillary acidic protein [GFAP]), oligodendrocyte (O4), and neuronal (TUJ1) markers revealed that IL-6 increased the proportion of tripotential neurospheres (Figure 4A4; 38.9% control versus 51.6% IL-6) to the detriment of bipotential neurospheres (Figure 4A4; 61.1% control versus 47.3% IL-6). This increase in multipotential cells raised the question whether IL-6 was inducing NSC differentiation toward producing more multipotential progenitors or whether IL-6 was directly affecting the proliferation of multipotential progenitors. To begin answering this question we reduced the cell density to generate clonal neurospheres. In contrast to the previous results, IL-6 treatment decreased neurosphere size but increased the number of the spheres (Figure 4B1–B3). Under these conditions, there was no increase in the relative number of tripotential neurospheres after IL-6 treatment (Figure 4B4; 33.3% control versus 27.6% IL-6), but an increase in monopotential neurospheres (Figure 4B4; 6.7% control versus 27.6% IL-6). These data suggest that the increase in multipotentiality previously observed was not driven by IL-6 directly affecting NSCs. Next, we grew neurospheres under 10 ng/mL FGF-2 and 10 ng/mL PDGF α , to reduce the number of NSCs in favor of PDGF-responsive progenitors. Under these conditions, IL-6 increased the number of neurospheres, while again reducing sphere size (Figure 4 C1–C3). IL-6 treatment also increased the number of tripotential neurospheres (Figure 4C4; 40% control versus 53.33% IL-6).

IL-6 Increases Proliferation of the PFMP *In Vitro*

To determine how IL-6 was affecting the proliferation of each progenitor and NSCs *in vitro*, we assessed EdU incorporation into the cultured SVZ NSPs using the multi-marker flow panel described above. SVZ NSPs were treated with 5 ng/mL of IL-6 + 5 ng/mL of sIL-6R for 10 h followed

by incubation with 10 μ M of EdU for 3 h (Figure 5A). The neurospheres were dissociated and analyzed by flow cytometry. Figures 5B–5D shows the gating strategy. Live cells were first gated for NG2⁺CD140a⁺, NG2⁺CD140a⁻, NG2⁻CD140a⁻. Next the NG2⁺CD140a⁺ were gated for CD133⁺LEX⁺, CD133⁻LEX⁺, CD133⁻LEX⁻ defined in our previous studies (Buono et al., 2012). We then applied the EdU gating to each population. IL-6 treatment increased the percentage of EdU⁺ PFMPs by 2-fold (Figure 5E; control: 7.98%; IL-6: 17.8%), whereas it decreased the percentage of GRP3 EdU⁺ cells (control: 27.4%; IL-6: 18.8%), BNAP EdU⁺ cells (control: 19.6%; IL-6: 13.6%), GRP2 EdU⁺ cells (control: 34.7%; IL-6: 21.3%), MP1 EdU⁺ cells (control: 20.4%; IL-6: 13.5%), and NSC EdU⁺ cells (control: 22.1%; IL-6: 12.6%) (Figures 5F–5J).

IL-6 Increases the Proportion of PFMPs *In Vitro*, at the Expense of NSCs and Other Progenitors

We used our multi-marker flow panel to establish how IL-6 affected the balance of the specific NSP subsets within the neurospheres. As above, NSPs were propagated as neurospheres in standard growth medium or medium supplemented with 5 ng/mL IL-6 + 5 ng/mL of sIL-6R. The proportion of subtypes was quantified by flow cytometry using: CD133/LeX/NG2/CD140a. A total of 20,000–40,000 live cell events were analyzed after excluding debris and dead cells using DAPI. Positively stained cells were classified by comparison with isotype controls. IL-6 significantly increased the percentage of PFMPs (control: 20.90% \pm 0.40%; IL-6: 31.90% \pm 0.20%) (Table 1; $p < 0.001$). However, it decreased the proportion of NSCs (control: 0.97% \pm 0.011%; IL-6: 0.79% \pm 0.027%; $p < 0.05$), MP1 (control: 4.65% \pm 0.03%; IL-6: 3.33% \pm 0.15%; $p < 0.001$), MP2s (control: 9.26% \pm 0.16%, IL-6: 7.44% \pm 0.10%; $p < 0.001$), BNAPs (control: 40.23% \pm 0.33%; IL-6: 34.6% \pm 0.45%; $p < 0.001$), GRP2s (control: 6.91% \pm 0.15%; IL-6: 5.76% \pm 0.030%; $p < 0.05$), and GRP3 (control: 5.75% \pm 0.12%; IL-6: 6.28% \pm 0.08%).

IL-6 Decreased the Output of Forebrain Astrocytes from the SVZ

After establishing that IL-6 modulated SVZ NSP proliferation, we asked whether increased levels of IL-6 would affect the production of neurons or astrocytes by performing fate mapping using an inducible Nestin-CreERT2/Rosa26-TdTomato reporter mouse. TdTomato expression was induced with 75 mg/kg tamoxifen injection at P1. Reporter mice were injected with 75 ng of IL-6 twice on P4 and once on P5. We evaluated TdTomato-expressing cells at P35 in those regions that would be receiving postnatally differentiating SVZ cells, such as the forebrain and olfactory bulbs, and compared cell numbers between IL-6-injected mice and PBS-injected controls. TdTomato⁺ cells exclusively

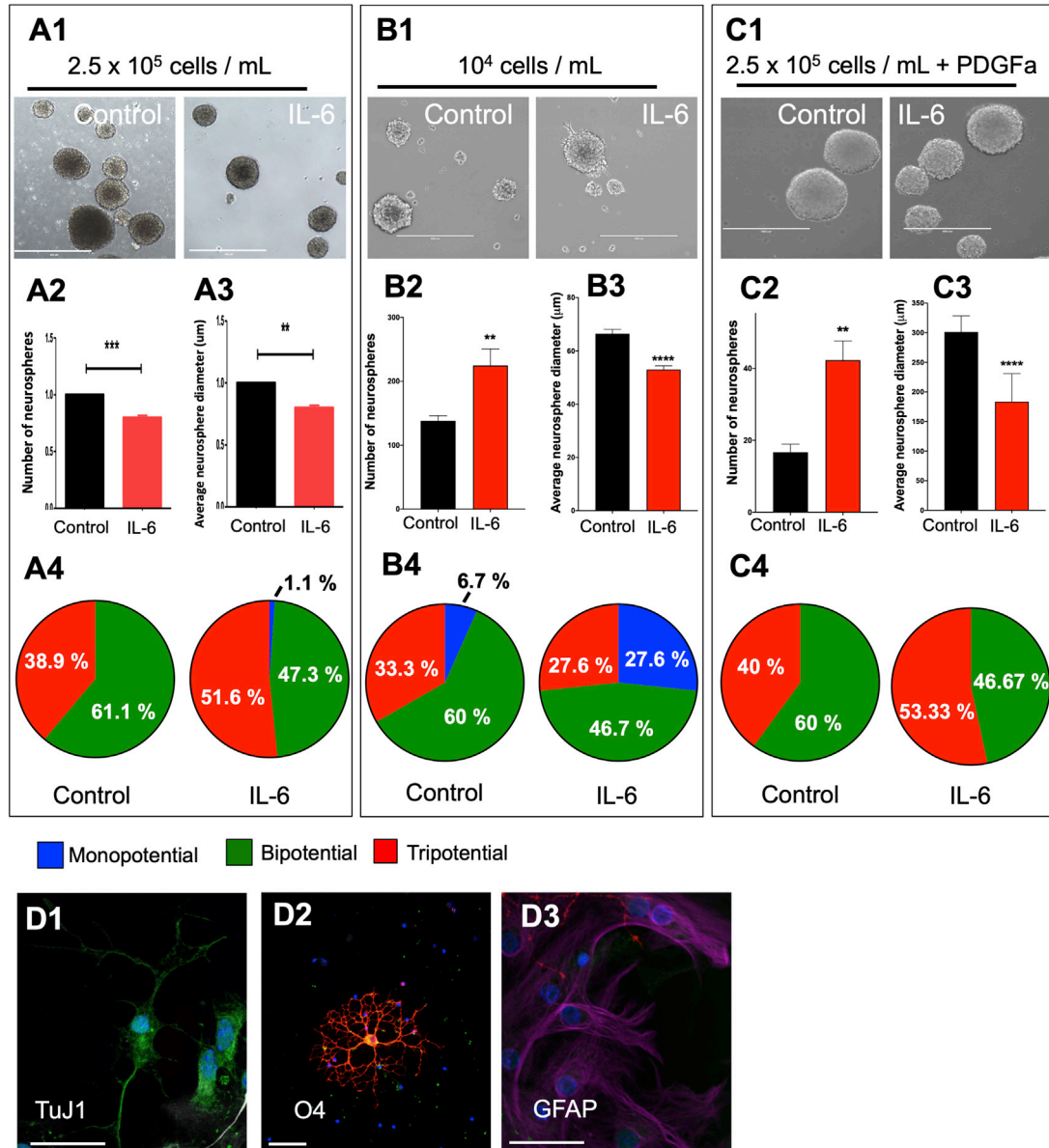
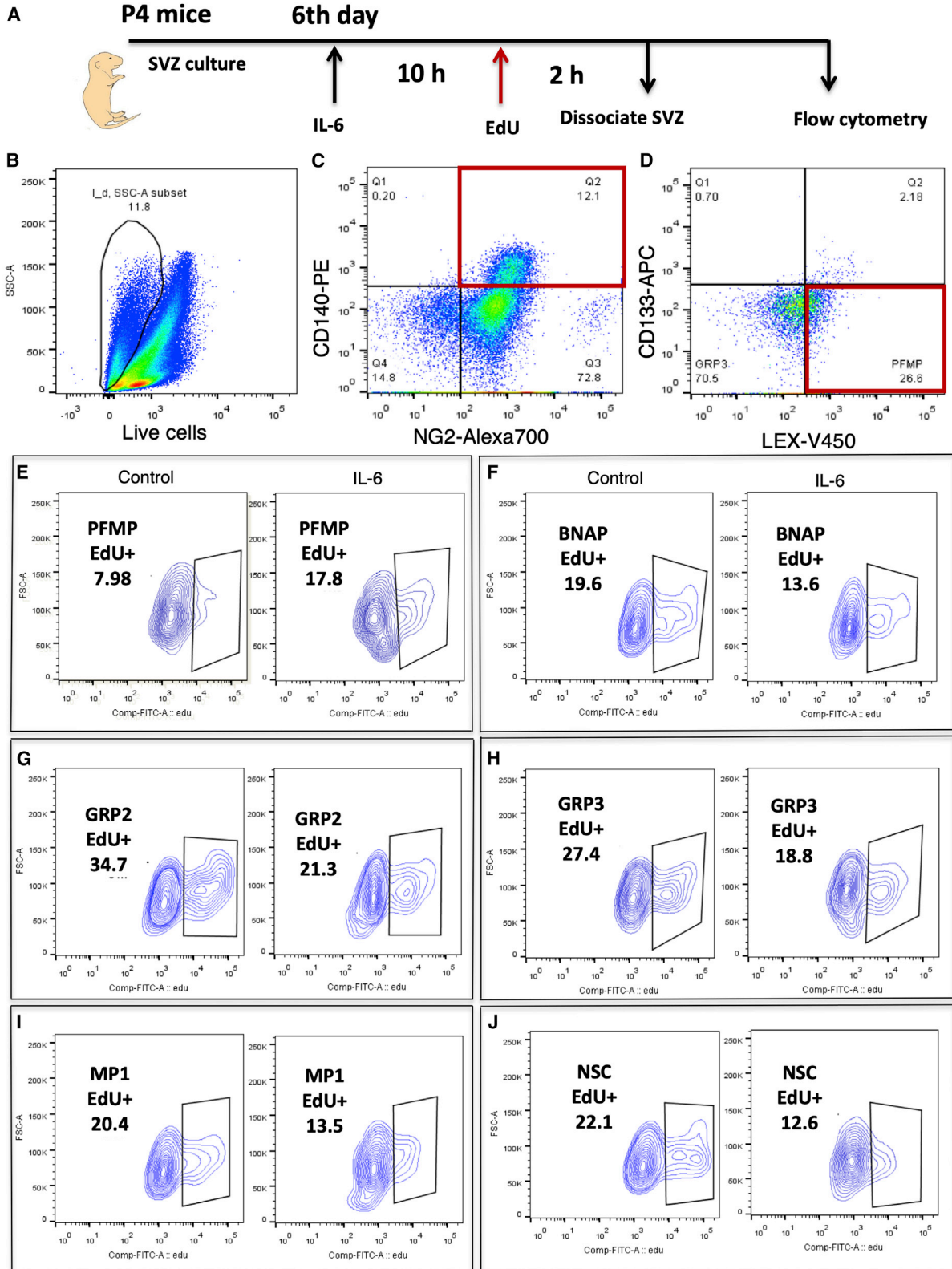


Figure 4. IL-6 Increases Tripotentiality in Neurospheres Containing PDGF-Responsive Progenitors, but Not in Neurospheres Enriched for NSCs

Secondary spheres were propagated in 20 ng/mL EGF + 10 ng/mL FGF-2 ± rmIL-6 (5 ng/mL) at different cell densities. (A1, B1, C1) Representative phase-contrast images of spheres from control and IL-6-treated groups at 7 days *in vitro* (DIV). Scale bars, 400 μm. Neurosphere number and average diameter were quantified at 7 DIV for neurospheres grown from 2.5 × 10⁵ (A2 and A3), 10⁴ (B2 and B3), and 2.5 × 10⁵ cells per mL + PDGFa (C2 and C3). Data are representative of three independent experiments with error bars representing mean ± SEM. At least 120 spheres were measured per group. ****p < 0.0001, **p < 0.01, versus control using Student unpaired t test. Neurospheres were differentiated and stained for TuJ1 (neurons) (D1), GFAP (astrocytes) (D2), and O4 (oligodendrocytes) (D3). Scale bars, 50 μm. Thirty spheres from each group were evaluated in each experiment to quantify the number of mono-, bi-, and tripotential spheres (A4, B4, C4). Data are representative of three independent experiments.

formed NeuN⁺ neurons in the granule cell layer of the olfactory bulb. However, IL-6 treatment had no effect in the number of those cells (Figures 6A and 6C). By contrast, IL-6-treated mice had ~50% fewer postnatally derived as-

trocytes in the frontal cortex (control: 0.23% ± 11.55%, n = 3; IL-6: 0.1% ± 8.74%, n = 4; p < 0.001) (Figures 6D and 6E), as demonstrated by positive staining for S-100b and negative staining for *Olig2* (Figure 6F).



(legend on next page)



Elevated Neonatal IL-6 Leads to an Olfaction Deficit in the Adult Mice

Although there was no difference in the numbers of new olfactory bulb neurons produced after IL-6 treatment, the possibility existed that the new neurons were inappropriately connected. Therefore, IL-6-treated mice were evaluated using the buried food test at P60 (Ziegler et al., 2019). This test revealed a significant deficit in olfaction, where the IL-6-injected animals had a 115% increase in latency in finding a sugary-flavored food compared with PBS-injected controls (171.9 versus 80.3; $p < 0.01$) (Figure 6B).

DISCUSSION

Many groups have reported an epidemiologic linkage between maternal infection during pregnancy with neurodevelopmental disorders in the offspring, including developmental delay, cerebral palsy, schizophrenia, and autism (Bear and Wu, 2016; Mednick et al., 1988; Zerbo et al., 2015), but how injury- or infection-induced inflammation affects fetal and neonatal brain development is poorly understood. Immune activators, such as LPS and poly(I:C), have been used in the animal models of MIA to highlight the importance of inflammatory cytokines (Shi et al., 2003; Smith et al., 2007). Specifically, the relative expression of pro- and anti-inflammatory cytokines in the fetal brain are important for the precise pathological profile emerging in later life. Several studies have clearly indicated that IL-6 is a key mediator of MIA and developmental problems in fetus. For example, one study suggested that a single injection of IL-6 into pregnant mice can mimic the effects of maternal infection on cognitive and behavioral disorders. Furthermore, administering a function-blocking antibody to IL-6 reversed the behavioral deficits induced by MIA in the poly(I:C) model (Smith et al., 2007). The importance of IL-6 is further supported in an LPS model of MIA, where administering the anti-inflammatory drug Pioglitazone abolished the increase in plasma IL-6 levels and ASD-like behaviors (Kirsten et al., 2018).

In the studies reported here we have begun to test the hypothesis that the proliferation and specification of NSCs and progenitors in the SVZ are altered as a causal component of the development of ASD. To model the increased

levels of IL-6 seen with antenatal infections, we established that intraperitoneal injections of 75 ng of IL-6 will increase blood plasma levels of IL-6 by 2-fold. As a consequence, the proliferation of PFMPs increased 2-fold. These multipotential progenitors are likely equivalent to the fetal PDGF-responsive precursors (PRPs) that were shown to be distinct from the NSCs (Chojnacki and Weiss, 2004). They are similar to the PRPs present in the neonatal rat SVZ as described by Moore et al. (2014). This unique and interesting population of neural progenitors has not been well studied. To determine whether IL-6 acts directly on the PFMPs and to establish the underlying mechanisms of action, we demonstrate that the PFMPs (as well as several other SVZ neural progenitors) express IL-6 α as well as GP130 receptors necessary for downstream IL-6 signaling pathways, and show that IL-6 activates pSTAT3 in these cells. The increased proliferation of PFMPs correlated with enhanced expression of the self-renewal gene *Fbxo15* and with decreased expression of *Tlx* (Nr2e1) and *Dnmt1*. Increased levels of IL-6 not only increased the proportion of PFMPs in the SVZ but also reduced the proportions of NSCs, MP1, BNAP/GRP1, and GRP2.

We postulated that the IL-6-mediated increase in PFMP proliferation could be due to increased expression of transcription factors involved in self-renewal of the neural progenitors. Therefore, we sorted PRPs, stimulated them with IL-6 and analyzed the expression of *Ascl1*, *Klf4*, *Id2*, *Olig2*, *Fbxo15*, *Tlx*, and *Gsx1*, which have been shown to be important for neural progenitor proliferation. Among those genes we saw an increase in *Fbxo15*, which interestingly, aside from being related to ESC self-renewal and proliferation (Okita et al., 2007), is associated with ASD in patients bearing 18q deletions (O'Donnell et al., 2010). We also found a highly significant decrease in the expression of *Tlx* (Nr2e1). In the hippocampus, *Tlx* promotes proliferation of neural progenitors (Shi et al., 2004) and NSCs (Murai et al., 2014; Niu et al., 2011). Consistent with our observation, *Tlx* was previously shown to be repressed by IL-1 β , impairing hippocampal neurogenesis and cognition (O'Leime et al., 2018b). Furthermore, *Tlx* null mice show reduced learning and memory (Zhang et al., 2008), associated with impaired synaptic plasticity (Christie et al., 2006), hippocampal neuroinflammation (Kozareva et al.,

Figure 5. IL-6 Increases PFMP Cell Proliferation and Decreases the Proliferation of NSCs and Other Progenitors *In Vitro*

SVZ neurospheres produced from P4 mice were treated with 5 ng/mL rmIL-6. After 10 h, 10 μ M EdU was added and 2 h later the cells were analyzed by flow cytometry using a multi-marker panel comprised of anti-CD133/LEX/NG2/CD140a followed by the Click-It reaction for EdU.

(A) Schematic of *in vitro* analysis of IL-6 effects on EdU incorporation in SVZ NSPs.

(B) Debris and dead cells were excluded using LIVE/DEAD blue.

(C and D) (C) After gating on CD140⁺/NG2⁺ cells this subset was separated based on intensity of CD133 and LeX (D).

Positively EdU stained cells were gated based on isotype control for PFMP (E), BNAP (F), GRP2 (G), GRP3 (H), MP1 (I) and NSC (J). Data are representative of two independent experiments conducted with triplicate technical replicates.

**Table 1. IL-6 Increases the Proportion of PDGF-Responsive Multipotent Progenitors at Expense of NSCs and Other Progenitors**

	NSC	PFMP	MP1	MP2	BNAP/GRP1	GRP3	GRP2
Control	0.97 ± 0.011 ^a	20.9 0 ± 0.40	4.65 ± 0.03	9.26 ± 0.16	40.23 ± 0.33	5.75 ± 0.12	6.91 ± 0.15
IL-6	0.79 ± 0.027*	31.90 ± 0.20***	3.33 ± 0.15***	7.44 ± 0.10***	34.60 ± 0.45***	6.28 ± 0.08	5.76 ± 0.08*

Data are the mean percentages for each SVZ NP ± SEM. *p < 0.05, **p < 0.01, ***p < 0.001.

^aData represent averages of three independent experiments.

2017), and decreased expression of synaptic genes (O’Leime et al., 2018a). These synaptic changes correlate with the observation that *Tlx* modulates ASD-relevant behaviors, such as anxiety and fear conditioning (O’Leary et al., 2016; Young et al., 2002).

A central gene controlling epigenetic regulation of gene transcription and chromatin structure, *Dnmt1*, has been reported to be increased in the brains of mice exposed to diesel exhaust during gestation. Diesel exhaust increases levels of IL-6 in the neonatal brain and produces behavioral outcomes reminiscent of ASD (Chang et al., 2019). In contrast, in our sorted PFMPs, we observed a complete ablation of *Dnmt1* expression. The role of DNMT1 in gliogenesis is complicated. Although DNA demethylation is necessary for STAT3 binding to the *Gfap* promoter, allowing NPCs to respond to astrocyte-inducing cytokines (Takizawa et al., 2001), silencing *Dnmt1* in ESCs is not sufficient to induce astroglial differentiation (Urayama et al., 2013). However, Fan et al., (2005) showed that suppressing *Dnmt1* in neural progenitors was sufficient to drive precocious astroglial differentiation through an increase in STAT signaling (Fan et al., 2005). By contrast, silencing *Dnmt1* in neocortical OPCs suppressed differentiation and induced cell damage (Egawa et al., 2019), suggesting that the mechanisms that control methylation are developmental and progenitor cell-type specific.

One suggested explanation for the diverse phenotype observed in ASD is attributed to the disruption of excitatory/inhibitory (E/I) circuit balance during critical periods of development. Neocortical GABAergic parvalbumin-positive inhibitory neurons, which normally drive experience-dependent circuit refinement, are crucial for critical period plasticity. Gogolla et al. (2009) showed that these interneurons were reduced in the neocortex across multiple genetic and non-genetic ASD mouse models (Gogolla et al., 2009), which would result in decreased numbers of inhibitory synapses. Interestingly, Wei et al. (2012) showed that intraventricular injections of IL-6 reduced the formation of inhibitory synapses and affected dendritic spine plasticity in a mouse model that exhibited an ASD-like behavioral phenotype (Wei et al., 2012).

The experimental paradigm used here is quite different from that used in previous MIA studies. For example, Galagher et al. (2013) provided IL-6 to pregnant mice at the

equivalent of the human early first trimester. Thus, their intervention would have affected neuroepithelial cells in the VZ. In contrast, we used neonatal mice to study the effects of increased level of IL-6 on SVZ NSPs at the human fetal equivalent of the beginning of the third trimester as it is this time that best correlates with the development of ASD (Zerbo et al., 2015). At this stage of development, the SVZ is expanding rapidly, giving rise to distinct sets of late-developing interneurons and glial progenitors that have been shown to be affected in ASD (Gogolla et al., 2009; Li et al., 2014; Marie et al., 2018).

We stably labeled postnatal NSCs to determine whether neonatal inflammation would affect the numbers or types of progeny that they produced in late-developing brain regions. An unexpected result was that olfactory bulb neurogenesis was unaffected in the IL-6-treated mice. In a recently published study, we evaluated SVZ neurogenesis after genetically deleting insulin growth factor II (IGF-II) in adulthood. We reported that this manipulation halved the SVZ NSC numbers, which resulted in an expansion in the progenitor cell pool and with increased numbers of neurons in the olfactory bulb (Ziegler et al., 2019). More recently we have obtained identical results by deleting the insulin receptor in the NSCs in adulthood (Chidambaram et al., in revision for *Stem Cell Reports*). As the newly added neurons in the olfactory bulb are inhibitory neurons, it was not surprising that the IGF-II and insulin receptor conditional null mice had deficits in olfaction. However, while neonatal IL-6 altered the composition of the SVZ NSP pool, there were no obvious differences in olfactory bulb neurogenesis, suggesting that the cause of the hypopsmia is more subtle.

What our fate mapping studies did reveal was a dramatic reduction in frontal neocortical astrocyte production. Changes in glial cell numbers, or in their state of activation, can subsequently increase or decrease synapse numbers (Allen and Eroglu, 2017). A seminal study by Muller and Best (1989) showed that transplanting newborn astrocytes into the adult brain could recover cortical synaptic plasticity in an ocular dominance model (Muller and Best, 1989). Therefore, a viable hypothesis is that reducing the numbers of astrocytes in the forebrain will upset the E/I synaptic balance producing long-lasting behavioral alterations. Supporting this hypothesis, a study that analyzed

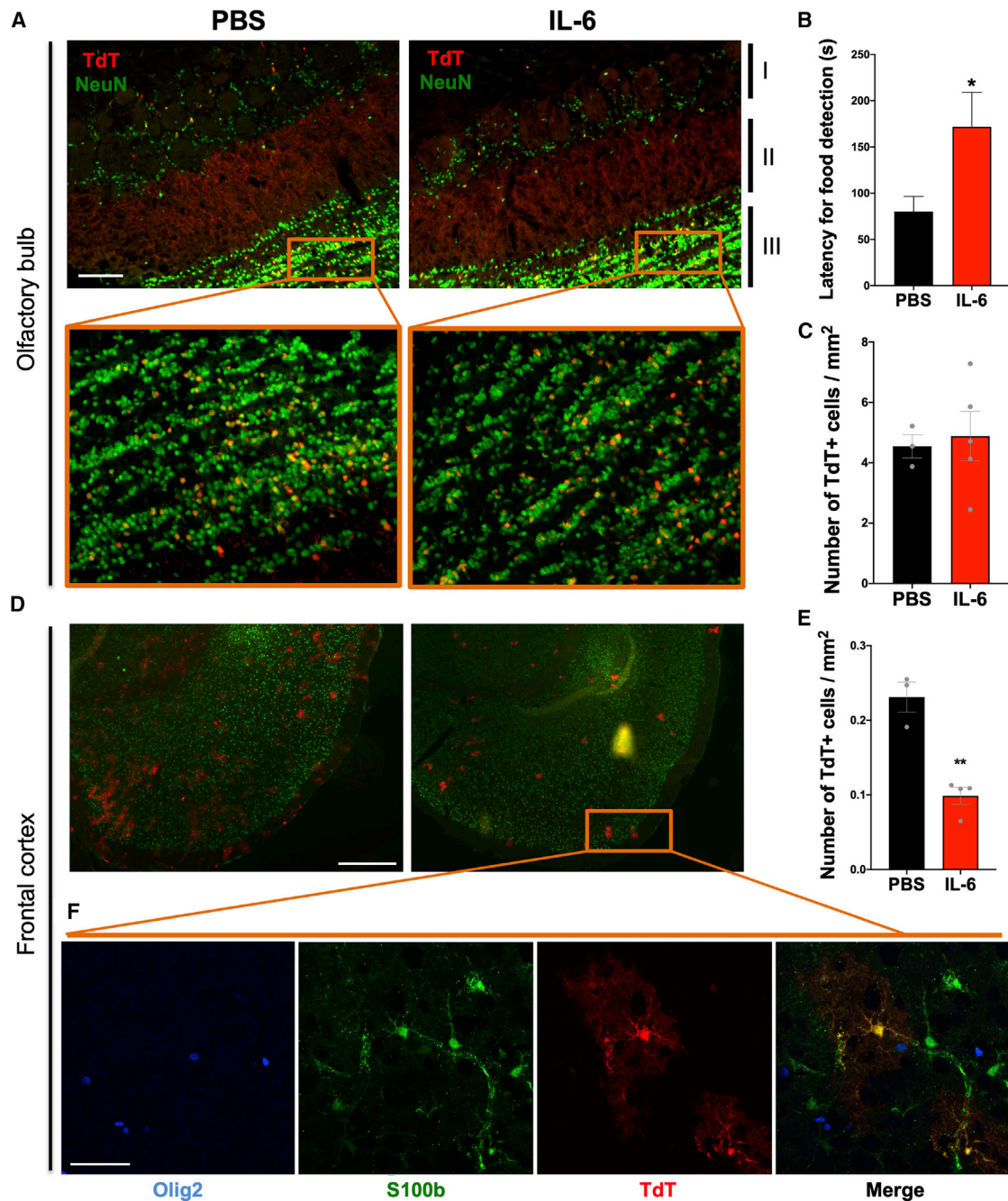


Figure 6. IL-6 Changes the Distribution of SVZ-Derived NSPs in Adult Mice Forebrain and Affects Olfaction

(A) Fluorescence for TdTomato+ (red) and NeuN+ (green) cells in the glomerular (I), mitral (II), and granule cell (III) layers of the olfactory bulb in IL-6-injected mice and PBS-injected controls. Scale bar, 100 μ m. The window shows double magnification.

(B) Buried food test. Latency to detect a hidden sugary food pellet (seconds). Error bars represent SEMs from three independent experiments. * $p < 0.05$ using Student's *t* test, comparing IL-6-treated samples with controls.

(C) Number of TdTomato+ cells per mm^2 in the granule cells layer (expanded detail window). Error bars represent SEMs from 3–5 mice per group.

(D) Frontal cortex from IL-6-injected and control mice showing TdTomato+ (red) and NeuN+ (green) cells. Scale bar, 500 μ m.

(E) Number of TdTomato+ cells per mm^2 in the frontal cortex. Error bars represent SEMs from 3–4 mice per group. * $p < 0.01$ using Student's *t* test.

(F) Confocal image showing co-expression of TdTomato+ and S100b+ cells in astrocytes, and no co-expression of *Olig2*+. Scale bar, 50 μ m.



a large cohort of ASD patient samples to identify ASD candidate genes found that the largest subset included many genes for synaptic transmission. Further analyses showed that many of those genes were involved in glial cell differentiation and were differentially expressed in the corpus callosum of ASD patients (Li et al., 2014).

The observation that neonatal IL-6 exposure reduced astrocyte production was somewhat surprising as earlier studies had shown that IL-6 promoted the differentiation of neocortical progenitors into oligodendrocytes and astrocytes (Bonni et al., 1997; Nakanishi et al., 2007). Islam et al. (2009) demonstrated that IL-6 signaling via STAT3 induced NSCs to differentiate into two types of astrocytes. Furthermore, our own earlier studies had shown that IL-6 synergizes with EGF to increase astrocyte proliferation (Levison et al., 2000). Here, we show that IL-6 reduced the abundance of two bipotential glial-restricted progenitors. Therefore, the most parsimonious explanation for the reduced numbers of astrocytes in the frontal lobe is that this was preceded by a loss in the numbers of these bipotential progenitors. At the present time there are no means to fate map these bipotential glial progenitors; however, we are in the process of validating unique markers for these cells based on an RNA sequencing analysis of FACS-purified SVZ progenitors so that these progenitors may be studied in more depth.

In their work, Gallagher et al. (2013) used the neurosphere assay and reported an increase in SVZ neurosphere-initiating cells cultured from adults exposed to IL-6 as fetuses. By contrast, in our experiments, when neurospheres were exposed to IL-6 *in vitro*, we observed a reduction of both sphere number and size. Our results also appear to conflict with those of Covey et al., (2011) who showed that IL-6 increased rat SVZ neurosphere number and size. They saw increased production of self-renewing, multipotent progenitors, which was interpreted as an increase in NSCs (Covey et al., 2011). However, neurosphere assays do not allow one to definitely conclude whether a stimulus is increasing the self-renewal and proliferation of NSCs or of multipotential progenitors since the neurosphere assay cannot distinguish between spheres formed by stem cells versus progenitors (Reynolds and Rietze, 2005). To address that question, we show that clonal neurospheres, which are predominantly formed from NSCs, do not show the same increase in potentiality when treated with IL-6. We also show that IL-6 is directly affecting the progenitors by showing that spheres cultured with FGF-2 and PDGF-A (a condition that is not permissive for NSC self-renewal [Chojnacki et al., 2011]), respond to IL-6 with an increase in the number of neuron-generating spheres. This experiment also argues against the conclusion that IL-6 promotes the differentiation of NSCs into tri-potential progenitors.

Our data suggest that the multipotential progenitors affected by IL-6 are probably PDGF responsive; however, different populations of multipotential PDGF-responsive progenitors exist in the postnatal SVZ. Therefore, we used a four-color flow cytometry panel, which can distinguish between eight different cell types found in the SVZ. Using this panel, we show that IL-6 increased the proportion of PFMPs, while simultaneously decreasing the proportion of NSCs within neurospheres *in vitro*. This result begins to explain how IL-6 treatment can reduce neurosphere number and size, while increasing multipotentiality. We also showed that IL-6 increased the percentage of EdU⁺ PFMPs by 2-fold compared with the decrease in EdU⁺ NSCs *in vitro* and we confirmed our *in vitro* results *in vivo* using intraperitoneal injections of IL-6, which increased the percentage of EdU⁺ PFMPs. We did not see any significant differences in NSC proliferation, but that can be attributed to long cell-cycle length of the NSCs, which was not captured as we evaluated a single time point. Altogether, these data lead to the conclusion that IL-6 expands the PFMPs at the expense of the NSCs.

It is becoming clear that different progenitor cell types are differentially responsive to IL-6 and that IL-6 can either promote or suppress cell proliferation. Monje et al. (2003) showed that the hippocampal neural progenitors expressed IL-6Rs and that an LPS challenge increased hippocampal IL-6R expression. They also showed that IL-6 inhibited hippocampal neurogenesis (Monje et al., 2003). Gallagher et al. (2013) showed IL-6R expression on Sox2⁺ VZ/SVZ precursors. Our flow cytometry data show that PFMP, MP2, GRP2, MP2, and BNAP express IL-6R α , whereas IL-6R α is not expressed by NSC, MP1, or GRP3. Those cell types that express membrane-bound IL-6R can be stimulated directly by IL-6, whereas the remainder can be stimulated by IL-6, but only through trans-signaling, which requires the sIL-6R α .

A number of signaling pathways have been shown to be activated by IL-6 in different CNS cell types, such as JAK and, to a lesser extent, TYK, which, in turn, activate downstream signaling proteins STATs. IL-6 can also activate the RAS-RAF-MAPK and the phosphatidylinositol 3-kinase pathways (Boulanger et al., 2003). Studies have investigated the activation of pSTAT1 versus pSTAT3 by IL-6 in highly enriched astrocyte compared with microglial cultures (Hsu et al., 2015). The astrocytes responded with significant increases in both pSTAT1 and pSTAT3, in contrast IL-6-treated microglia activated pSTAT1 significantly, but not pSTAT3. Therefore, we evaluated signal transduction pathways activated in SVZ NSPs in response to IL-6. We found a significant increase in pSTAT3 signal, but not in pSTAT1, in response to IL-6 and no effect on either pAKT or p44/p42 MAPK. Interestingly, LIF activated both STAT1 and STAT3.



Altogether our studies show that increased blood levels of IL-6 dysregulate the NSPs of the mouse SVZ, increasing PFMP proliferation while simultaneously decreasing the percentage of NSCs as well as two bipotential glial-restricted progenitors. This shift in the composition of the forebrain germinal zone progenitors is accompanied by changes in gliogenesis as well as in olfactory sensitivity. Altogether, these studies provide important new insights into the molecular and cellular underpinnings of neurodevelopmental disorders associated with maternal infections.

EXPERIMENTAL PROCEDURES

Materials

Common laboratory chemicals were purchased from either Sigma or VWR. Cell culture media and supplements were purchased from Invitrogen or Sigma.

Mice

C57BL/6 mice were generated in-house from mice purchased from Jackson Laboratory (Bar Harbor, ME). C57BL/6 mice were used for neurosphere studies, western blot analyses, and flow cytometry. Swiss Webster mice from time-pregnant females purchased from Charles River laboratories were used for all *in vivo* studies. Only male mice were used for *in vivo* EdU experiments, as ASD is most prevalent in males. All experiments were performed in accordance with protocol 17,064 approved by the IACUC committee of Rutgers University Biomedical Health Sciences.

IL-6 Injections and ELISA

P4 Swiss Webster mice were injected twice intraperitoneally with PBS or carrier-free rmIL-6 (R&D Systems, Minneapolis, MN) using a Hamilton syringe separated by 8 h. Trunk blood was collected in 100 USP of Heparin Sodium (Sagent Pharmaceuticals, Schaumburg, IL) 2 h after injection. Samples were centrifuged at $2,000 \times g$ for 15 min and then aliquoted and stored at -80°C until analyzed. A mouse IL-6 ELISA Kit (BD OptEIA) was used to analyze the samples.

Neurosphere Experiments

Neural progenitors were cultured from SVZs of 4–7-day-old C57BL/6 mice as described previously (Buono et al., 2015). Culture plates for secondary neurospheres were seeded with 2.5×10^5 or 10^4 cells per mL. Total neurosphere numbers were counted for each experimental replicate under an inverted microscope. Neurosphere diameter was calculated using Zeiss Axiovision and ImageJ software. Cell yield was counted by trypan blue exclusion. Neurospheres were differentiated as described previously and stained for β -tubulin III (TUJ1, 1:300; Covance, Princeton, NJ), GFAP (1:500; Dako, Carpinteria, CA), and O4 (produced in-house). Secondary antibodies included goat anti-mouse IgG2a dylight 488 for TUJ1, goat anti-mouse IgG dylight 549 for GFAP, and goat anti-mouse IgM dylight 647 (Jackson ImmunoResearch, West Grove, PA). Images of stained cells were collected using a Q-imaging Retiga CCD camera (Surrey, BC, Canada) interfaced with iVision scientific

imaging software (Scanalytics) on an Olympus AX-70 microscope (Olympus, NJ).

Flow Cytometry Gating

Flow cytometry was performed as described by Buono et al. (2015) using the following antibodies specified in Tables S3 and S4. Lewis-X (1/20; BD Biosciences), CD133-APC (1/50; eBioscience), CD140a (1/400; BioLegend), and NG2 chondroitin sulfate proteoglycan (1/50; Millipore). EdU experiments were performed as described previously (Chen et al., 2015). Goat anti-rabbit IgG Alexa Fluor 700 (1/100; Invitrogen) was used for NG2. DAPI was used for dead cell exclusion. IL-6R α was analyzed using the flow panel described above with the addition of an antibody against IL-6R α (1/20, R&D Systems). All sample data were collected on a BD LSR II (BD Biosciences) and analyzed using FlowJo.

Quantitative Real-Time PCR Analysis

SVZ NSPs were propagated as neurospheres in medium supplemented with 20 ng/mL EGF and 10 ng/mL FGF-2. Neurospheres were dissociated, propagated for 4 days, and PFMPs were sorted using FACS. Sorted cells were cultured in the absence or presence of rmIL-6 (5 ng/mL) + sIL-6R (5 ng/mL) for 2 h. RNA was isolated using NucleoSpin RNA Plus Kit (Macherey-Nagel), amplified and cDNA generated using iScript cDNA synthesis kit (Bio-Rad). qPCR was performed using 100 ng of cDNA and validated QuantiTect SYBR Green primers (QIAGEN) on an CFX 96 real-time PCR system (Bio-Rad). 18S RNA and actb were used as normalization controls. Relative quantification was evaluated by the $\Delta\Delta$ Ct method.

Western Blots

Exponentially growing cultures of neural progenitors were treated \pm IL-6/sIL-6R for 30 min and harvested at the indicated time points. The cells were washed with ice-cold PBS, then placed into lysis buffer (50 mM Tris-HCl [pH 7.6], 50 mM NaCl, 0.1% sodium dodecyl sulfate, 1% Triton X-100) and protease inhibitors. The lysates were sonicated, then clarified by centrifugation at $10,000 \times g$ at 4°C for 15 min. Aliquots of 30–50 μg of protein of lysate were fractionated on 4%–12% SDS-polyacrylamide gels and transferred to nitrocellulose membranes. The blots were developed using antibodies to the phosphorylated and non-phosphorylated forms of the following signal transduction proteins: pSTAT3, pSTAT1, MAPK, and AKT (all from Cell Signaling Technology, Danvers, MA). Independent experiments were repeated at least three times. For IL-6R expression, RAW 264.7 cell lysate was used as a positive control. Blots were developed for IL-6R α and for GP130 (antibodies from R&D Systems) followed by chemiluminescent detection using Western Lightning Plus-ECL (PerkinElmer, Waltham, MA) and ChemiDoc Touch imaging system (Bio-Rad).

Statistical Analyses

For all datasets, statistical analyses were performed using Student's unpaired t test and ANOVA followed by Tukey's *post-hoc* multiple comparison test. A $p < 0.05$ was considered significant. In figures, asterisks denote statistical significance marked by * $p < 0.05$, ** $p < 0.01$, *** $p < 0.001$. GraphPad Prism (version 5.01) was used for all analyses. Sample sizes (n) are indicated in the figure legends.



SUPPLEMENTAL INFORMATION

Supplemental Information can be found online at <https://doi.org/10.1016/j.stemcr.2020.03.019>.

AUTHOR CONTRIBUTIONS

E.K. and F.J.V. performed most of the experiments, data analysis, and wrote the manuscript. A.N. performed some neurosphere culture and analysis. V.H.S. and K.D.B. contributed to flow cytometry experiments. All authors reviewed the manuscript. S.W.L. participated in the design of the experiments, supervised the execution of the experiments, oversaw the data analysis, and participated in writing the manuscript.

ACKNOWLEDGMENTS

This work was supported by a grant from the Governor's Council for Medical Research and Treatment of Autism, CAUT17BSP010 and by an NIH R21, NS107772 awarded to S.W.L.

Received: October 18, 2018

Revised: March 17, 2020

Accepted: March 18, 2020

Published: April 16, 2020

REFERENCES

- Aaltonen, R., Heikkinen, T., Hakala, K., Laine, K., and Alanen, A. (2005). Transfer of proinflammatory cytokines across term placenta. *Obstet. Gynecol.* *106*, 802–807.
- Allen, N.J., and Eroglu, C. (2017). Cell biology of astrocyte-synapse interactions. *Neuron* *96*, 697–708.
- Ashwood, P., Krakowiak, P., Hertz-Picciotto, I., Hansen, R., Pessah, I., and Van de Water, J. (2011). Elevated plasma cytokines in autism spectrum disorders provide evidence of immune dysfunction and are associated with impaired behavioral outcome. *Brain Behav. Immun.* *25*, 40–45.
- Atladottir, H.O., Thorsen, P., Ostergaard, L., Schendel, D.E., Lemcke, S., Abdallah, M., and Parner, E.T. (2010). Maternal infection requiring hospitalization during pregnancy and autism spectrum disorders. *J. Autism Dev. Disord.* *40*, 1423–1430.
- Bear, J.J., and Wu, Y.W. (2016). Maternal infections during pregnancy and cerebral palsy in the child. *Pediatr. Neurol.* *57*, 74–79.
- Bonni, A., Sun, Y., Nadal-Vicens, M., Bhatt, A., Frank, D.A., Rozovsky, I., Stahl, N., Yancopoulos, G.D., and Greenberg, M.E. (1997). Regulation of gliogenesis in the central nervous system by the JAK-STAT signaling pathway. *Science* *278*, 477–483.
- Boulanger, M.J., Chow, D.C., Brevnova, E.E., and Garcia, K.C. (2003). Hexameric structure and assembly of the interleukin-6/IL-6 alpha-receptor/gp130 complex. *Science* *300*, 2101–2104.
- Buono, K.D., Goodus, M.T., Guardia Clausi, M., Jiang, Y., Loporchio, D., and Levison, S.W. (2015). Mechanisms of mouse neural precursor expansion after neonatal hypoxia-ischemia. *J. Neurosci.* *35*, 8855–8865.
- Buono, K.D., Vadlamuri, D., Gan, Q., and Levison, S.W. (2012). Leukemia inhibitory factor is essential for subventricular zone neural stem cell and progenitor homeostasis as revealed by a novel flow cytometric analysis. *Dev. Neurosci.* *34*, 449–462.
- Chang, Y.C., Daza, R., Hevner, R., Costa, L.G., and Cole, T.B. (2019). Prenatal and early life diesel exhaust exposure disrupts cortical lamina organization: evidence for a reelin-related pathogenic pathway induced by interleukin-6. *Brain Behav Immun* *78*, 105–115.
- Chen, H., Goodus, M., de Toledo, S., Azzam, E., Levison, S., and Souayah, N. (2015). Ionizing radiation perturbs cell cycle progression of neural precursors in the subventricular zone without affecting their long-term self-renewal. *ASN Neuro* *2015*, 1–16.
- Chojnacki, A., Mak, G., and Weiss, S. (2011). PDGFRalpha expression distinguishes GFAP-expressing neural stem cells from PDGF-responsive neural precursors in the adult periventricular area. *J. Neurosci.* *31*, 9503–9512.
- Chojnacki, A., and Weiss, S. (2004). Isolation of a novel platelet-derived growth factor-responsive precursor from the embryonic ventral forebrain. *J. Neurosci.* *24*, 10888–10899.
- Christie, B.R., Li, A.M., Redila, V.A., Booth, H., Wong, B.K., Eadie, B.D., Ernst, C., and Simpson, E.M. (2006). Deletion of the nuclear receptor Nr2e1 impairs synaptic plasticity and dendritic structure in the mouse dentate gyrus. *Neuroscience* *137*, 1031–1037.
- Covey, M.V., Loporchio, D., Buono, K.D., and Levison, S.W. (2011). Opposite effect of inflammation on subventricular zone versus hippocampal precursors in brain injury. *Ann. Neurol.* *70*, 616–626.
- Croonenberghs, J., Bosmans, E., Deboutte, D., Kenis, G., and Maes, M. (2002). Activation of the inflammatory response system in autism. *Neuropsychobiology* *45*, 1–6.
- Egawa, N., Shindo, A., Hikawa, R., Kinoshita, H., Liang, A.C., Itoh, K., Lok, J., Maki, T., Takahashi, R., Lo, E.H., et al. (2019). Differential roles of epigenetic regulators in the survival and differentiation of oligodendrocyte precursor cells. *Glia* *67*, 718–728.
- Fan, G., Martinowich, K., Chin, M.H., He, F., Fouse, S.D., Hutnick, L., Hattori, D., Ge, W., Shen, Y., Wu, H., et al. (2005). DNA methylation controls the timing of astroglialogenesis through regulation of JAK-STAT signaling. *Development* *132*, 3345–3356.
- Gallagher, D., Norman, A.A., Woodard, C.L., Yang, G., Gauthier-Fisher, A., Fujitani, M., Vessey, J.P., Cancino, G.I., Sachewsky, N., Woltjen, K., et al. (2013). Transient maternal IL-6 mediates long-lasting changes in neural stem cell pools by deregulating an endogenous self-renewal pathway. *Cell Stem Cell* *13*, 564–576.
- Gogolla, N., Leblanc, J.J., Quast, K.B., Sudhof, T.C., Fagiolini, M., and Hensch, T.K. (2009). Common circuit defect of excitatory-inhibitory balance in mouse models of autism. *J. Neurodev Disord.* *1*, 172–181.
- Gomez, R., Romero, R., Ghezzi, F., Yoon, B.H., Mazor, M., and Berry, S.M. (1998). The fetal inflammatory response syndrome. *Am. J. Obstet. Gynecol.* *179*, 194–202.
- Hsu, M.-P., Frausto, R., Rose-John, S., and Campbell, I.L. (2015). Analysis of IL-6/gp130 family receptor expression reveals that in contrast to astroglia, microglia lack the oncostatin M receptor and functional responses to oncostatin M. *Glia* *63*, 132–141.
- Islam, O., Gong, X., Rose-John, S., and Heese, K. (2009). Interleukin-6 and neural stem cells: more than gliogenesis. *Mol. Biol. Cell* *20*, 188–189.



- Kirsten, T.B., Casarin, R.C., Bernardi, M.M., and Felicio, L.F. (2018). Pioglitazone abolishes autistic-like behaviors via the IL-6 pathway. *PLoS One* 13, e0197060.
- Kozareva, D.A., Hueston, C.M., O'Leime, C.S., Crotty, S., Dockery, P., Cryan, J.F., and Nolan, Y.M. (2017). Absence of the neurogenesis-dependent nuclear receptor TLX induces inflammation in the hippocampus. *J. Neuroimmunol* 331, 87–96.
- Lee, B.K., Magnusson, C., Gardner, R.M., Blomstrom, A., Newschaffer, C.J., Burstyn, I., Karlsson, H., and Dalman, C. (2015). Maternal hospitalization with infection during pregnancy and risk of autism spectrum disorders. *Brain Behav. Immun.* 44, 100–105.
- Levison, S.W., Jiang, F.J., Stoltzfus, O.K., and Ducceschi, M.H. (2000). IL-6-type cytokines enhance epidermal growth factor-stimulated astrocyte proliferation, [In Process Citation]. *Glia* 32, 328–337.
- Li, J., Shi, M., Ma, Z., Zhao, S., Euskirchen, G., Ziskin, J., Urban, A., Hallmayer, J., and Snyder, M. (2014). Integrated systems analysis reveals a molecular network underlying autism spectrum disorders. *Mol. Syst. Biol.* 10, 774.
- Malkova, N.V., Yu, C.Z., Hsiao, E.Y., Moore, M.J., and Patterson, P.H. (2012). Maternal immune activation yields offspring displaying mouse versions of the three core symptoms of autism. *Brain Behav. Immun.* 26, 607–616.
- Marie, C., Clavairoly, A., Frah, M., Hmidan, H., Yan, J., Zhao, C., Van Steenwinckel, J., Daveau, R., Zalc, B., Hassan, B., et al. (2018). Oligodendrocyte precursor survival and differentiation requires chromatin remodeling by Chd7 and Chd8. *Proc. Natl. Acad. Sci. U S A* 115, E8246–E8255.
- Mednick, S.A., Machon, R.A., Huttunen, M.O., and Bonett, D. (1988). Adult schizophrenia following prenatal exposure to an influenza epidemic. *Arch. Gen. Psychiatry* 45, 189–192.
- Meyer, U., Nyffeler, M., Engler, A., Urwyler, A., Schedlowski, M., Knuesel, I., Yee, B.K., and Feldon, J. (2006). The time of prenatal immune challenge determines the specificity of inflammation-mediated brain and behavioral pathology. *J. Neurosci.* 26, 4752–4762.
- Monje, M.L., Toda, H., and Palmer, T.D. (2003). Inflammatory blockade restores adult hippocampal neurogenesis. *Science* 302, 1760–1765.
- Moore, L., Bain, J.M., Loh, J.M., and Levison, S.W. (2014). PDGF-responsive progenitors persist in the subventricular zone across the lifespan. *ASN Neuro* 6. <https://doi.org/10.1042/AN20120041>.
- Muller, C.M., and Best, J. (1989). Ocular dominance plasticity in adult cat visual cortex after transplantation of cultured astrocytes. *Nature* 342, 427–430.
- Murai, K., Qu, Q., Sun, G., Ye, P., Li, W., Asuelime, G., Sun, E., Tsai, G.E., and Shi, Y. (2014). Nuclear receptor TLX stimulates hippocampal neurogenesis and enhances learning and memory in a transgenic mouse model. *Proc. Natl. Acad. Sci. U S A* 111, 9115–9120.
- Nakanishi, M., Niidome, T., Matsuda, S., Akaike, A., Kihara, T., and Sugimoto, H. (2007). Microglia-derived interleukin-6 and leukaemia inhibitory factor promote astrocytic differentiation of neural stem/progenitor cells. *Eur. J. Neurosci.* 25, 649–658.
- Niu, W., Zou, Y., Shen, C., and Zhang, C.L. (2011). Activation of postnatal neural stem cells requires nuclear receptor TLX. *J. Neurosci.* 31, 13816–13828.
- O'Donnell, L., Soileau, B., Heard, P., Carter, E., Sebold, C., Gelfond, J., Hale, D.E., and Cody, J.D. (2010). Genetic determinants of autism in individuals with deletions of 18q. *Hum. Genet.* 128, 155–164.
- O'Leary, J.D., Kozareva, D.A., Hueston, C.M., O'Leary, O.F., Cryan, J.F., and Nolan, Y.M. (2016). The nuclear receptor Tlx regulates motor, cognitive and anxiety-related behaviours during adolescence and adulthood. *Behav. Brain Res.* 306, 36–47.
- O'Leime, C.S., Hoban, A.E., Hueston, C.M., Stilling, R., Moloney, G., Cryan, J.F., and Nolan, Y.M. (2018a). The orphan nuclear receptor TLX regulates hippocampal transcriptome changes induced by IL-1beta. *Brain Behav. Immun.* 70, 268–279.
- O'Leime, C.S., Kozareva, D.A., Hoban, A.E., Long-Smith, C.M., Cryan, J.F., and Nolan, Y.M. (2018b). TLX is an intrinsic regulator of the negative effects of IL-1beta on proliferating hippocampal neural progenitor cells. *FASEB J.* 32, 613–624.
- Okita, K., Ichisaka, T., and Yamanaka, S. (2007). Generation of germline-competent induced pluripotent stem cells. *Nature* 448, 313–317.
- Reynolds, B.A., and Rietze, R.L. (2005). Neural stem cells and neurospheres—re-evaluating the relationship. *Nat. Methods* 2, 333–336.
- Salmaso, N., Jablonska, B., Scafidi, J., Vaccarino, F.M., and Gallo, V. (2014). Neurobiology of premature brain injury. *Nat. Neurosci.* 17, 341–346.
- Shi, L., Fatemi, S.H., Sidwell, R.W., and Patterson, P.H. (2003). Maternal influenza infection causes marked behavioral and pharmacological changes in the offspring. *J. Neurosci.* 23, 297–302.
- Shi, Y., Chichung Lie, D., Taupin, P., Nakashima, K., Ray, J., Yu, R.T., Gage, F.H., and Evans, R.M. (2004). Expression and function of orphan nuclear receptor TLX in adult neural stem cells. *Nature* 427, 78–83.
- Smith, S.E., Li, J., Garbett, K., Mirnics, K., and Patterson, P.H. (2007). Maternal immune activation alters fetal brain development through interleukin-6. *J. Neurosci.* 27, 10695–10702.
- Takizawa, T., Nakashima, K., Namihira, M., Ochiai, W., Uemura, A., Yanagisawa, M., Fujita, N., Nakao, M., and Taga, T. (2001). DNA methylation is a critical cell-intrinsic determinant of astrocyte differentiation in the fetal brain. *Dev. Cell* 1, 749–758.
- Urayama, S., Semi, K., Sanosaka, T., Hori, Y., Namihira, M., Kohyama, J., Takizawa, T., and Nakashima, K. (2013). Chromatin accessibility at a STAT3 target site is altered prior to astrocyte differentiation. *Cell Struct. Funct.* 38, 55–66.
- Wei, H., Chadman, K.K., McCloskey, D.P., Sheikh, A.M., Malik, M., Brown, W.T., and Li, X. (2012). Brain IL-6 elevation causes neuronal circuitry imbalances and mediates autism-like behaviors. *Biochim. Biophys. Acta* 1822, 831–842.
- Wu, W.L., Hsiao, E.Y., Yan, Z., Mazmanian, S.K., and Patterson, P.H. (2017). The placental interleukin-6 signaling controls fetal brain development and behavior. *Brain Behav. Immun.* 62, 11–23.



Yang, C.J., Liu, C.L., Sang, B., Zhu, X.M., and Du, Y.J. (2015). The combined role of serotonin and interleukin-6 as biomarker for autism. *Neuroscience* 284, 290–296.

Young, K.A., Berry, M.L., Mahaffey, C.L., Saionz, J.R., Hawes, N.L., Chang, B., Zheng, Q.Y., Smith, R.S., Bronson, R.T., Nelson, R.J., et al. (2002). Fierce: a new mouse deletion of Nr2e1; violent behaviour and ocular abnormalities are background-dependent. *Behav. Brain Res.* 132, 145–158.

Zaretsky, M.V., Alexander, J.M., Byrd, W., and Bawdon, R.E. (2004). Transfer of inflammatory cytokines across the placenta. *Obstet. Gynecol.* 103, 546–550.

Zerbo, O., Qian, Y., Yoshida, C., Grether, J.K., Van de Water, J., and Croen, L.A. (2015). Maternal infection during pregnancy and autism spectrum disorders. *J. Autism Dev. Disord.* 45, 4015–4025.

Zhang, C.L., Zou, Y., He, W., Gage, F.H., and Evans, R.M. (2008). A role for adult TLX-positive neural stem cells in learning and behaviour. *Nature* 451, 1004–1007.

Ziegler, A.N., Feng, Q., Chidambaram, S., Testai, J.M., Kumari, E., Rothbard, D.E., Constancia, M., Sandovici, I., Cominski, T., Pang, K., et al. (2019). Insulin-like growth factor II: an essential adult stem cell niche constituent in brain and intestine. *Stem Cell Reports* 12, 816–830.